

Kink-antikink unbinding transition in the two-dimensional fully frustrated XY model

 Peter Olsson¹ and S. Teitel²
¹*Department of Theoretical Physics, Umeå University, 901 87 Umeå, Sweden*
²*Department of Physics and Astronomy, University of Rochester, Rochester, New York 14627, USA*

(Received 27 December 2004; published 29 March 2005)

We carry out numerical simulations to directly confirm the existence of a kink-antikink unbinding transition along Ising-like domain walls in the two-dimensional fully frustrated XY model. We comment on the possible implications of kink-antikink unbinding for the bulk phase transition of the model.

DOI: 10.1103/PhysRevB.71.104423

PACS number(s): 75.10.-b, 64.60.-i, 74.50.+r

I. INTRODUCTION

The two-dimensional (2D) fully frustrated XY (FFXY) model^{1,2} is one of the most intriguing of the “simple” statistical mechanics models. The doubly degenerate checkerboard pattern of vortices in the ground state leads to an Ising-like discrete $Z(2)$ symmetry in addition to the Kosterlitz-Thouless-like continuous $O(2)$ symmetry associated with the uniform rotation of all phase angles.³ It remains controversial whether there are two distinct phase transitions $T_{KT} < T_I$, with T_{KT} marking the breaking of the $O(2)$ symmetry and T_I marking the breaking of the $Z(2)$ symmetry,⁴⁻⁶ or, rather, a single transition in which both symmetries are broken simultaneously.⁷

Recently, Korshunov⁸ presented an argument for a new interfacial transition T_w in the 2D FFX model, lying well below the bulk transition(s), arising from the unbinding of step excitations of unit height (“kink-antikink pairs”) on the domain walls associated with the $Z(2)$ symmetry. Korshunov argued that the kink-antikink unbinding transition leads to a decoupling of phase coherence across domain boundaries, supporting the identification of the FFX with the coupled XY-Ising model.⁹ Korshunov further argued that this effect necessarily leads to the scenario of two distinct bulk transitions, $T_{KT} < T_I$.

Earlier, Lee and co-workers, first in simulations of the 2D FFX model with Langevin dynamics,¹⁰ and then in its dual Coulomb gas (CG) model with Monte Carlo (MC) dynamics,¹¹ found evidence for a transition in domain wall morphology in simulations of the ordering kinetics of domain growth following a sudden quench. They interpreted this as a finite-temperature roughening transition of the Ising-like domain walls. Jeon *et al.*¹² made similar conclusions in simulations of the 2D FFX with resistively shunted junction dynamics. Korshunov,⁸ however, has argued that domain walls should be rough at all temperatures.

In this paper we present direct numerical evidence demonstrating the existence of the kink-antikink unbinding transition at a temperature T_w below the bulk transition(s). In agreement with Korshunov’s predictions, we show that phase angles on opposite sides of the domain wall decouple above T_w . The numerical value we find for T_w is comparable to that of the morphological transition found by Lee *et al.*,¹¹ however, we explicitly demonstrate that the domain walls are rough at temperatures well below T_w . This indicates that the transition seen by Lee and co-workers was really kink-antikink unbinding, rather than roughening.

II. THE MODEL

A. The fully frustrated XY model

We study the 2D FFX model on a square lattice, given by the Hamiltonian,^{1,2}

$$\mathcal{H}[\theta(\mathbf{r}_i)] = \sum_{i,\mu} V[\theta(\mathbf{r}_i + \hat{\mu}) - \theta(\mathbf{r}_i) - A_\mu(\mathbf{r}_i)]. \quad (1)$$

Here $\theta(\mathbf{r}_i)$ is the thermally fluctuating phase angle of the planar XY spin on site $\mathbf{r}_i = x_i \hat{x} + y_i \hat{y}$ (x_i, y_i integers) of a $L_x \times L_y$ periodic square lattice, $\hat{\mu} = \hat{x}, \hat{y}$ labels the bond directions of the lattice, and $A_\mu(\mathbf{r}_i)$ is the quenched gauge field on the bond leaving site \mathbf{r}_i in direction $\hat{\mu}$ [with $A_{-\mu}(\mathbf{r}_i + \hat{\mu}) \equiv -A_\mu(\mathbf{r}_i)$]. For full frustration, the $A_\mu(\mathbf{r}_i)$ are constrained so that their directed sum going counterclockwise around any plaquette P of the lattice is fixed (modulus 2π) to

$$\sum_P A_\mu(\mathbf{r}_i) = \pi. \quad (2)$$

To implement the constraint of Eq. (2), we use the specific gauge choice,

$$A_x(\mathbf{r}_i) = 0, \quad A_y(\mathbf{r}_i) = (-1)^{x_i}(\pi/2). \quad (3)$$

The interaction potential $V(\phi)$ is periodic on $(0, 2\pi)$, with a single quadratic minimum at $\phi=0$. We will take for $V(\phi)$ the commonly used Villain function,¹³

$$V(\phi) = -T \ln \left[\sum_{m=-\infty}^{\infty} e^{-J(\phi - 2\pi m)^2/2T} \right]. \quad (4)$$

The boundary conditions for the phase angles are, in the most general case, given by^{14,15}

$$\theta(\mathbf{r}_i + L_\mu \hat{\mu}) - \theta(\mathbf{r}_i) = \Delta_\mu, \quad (5)$$

where $\Delta_\mu \in [0, 2\pi)$ is the total twist applied across the system in direction $\hat{\mu}$. $\Delta_\mu=0$ corresponds to periodic boundary conditions. Alternatively, if one makes the change of variables, $\theta'(\mathbf{r}_i) \equiv \theta(\mathbf{r}_i) - \mathbf{r}_i \cdot \mathbf{d}$, with $d_\mu \equiv \Delta_\mu/L_\mu$, then the system has periodic boundary conditions in the $\theta'(\mathbf{r}_i)$ and the applied twist appears as an additive constant to the gauge field, $A_\mu(\mathbf{r}_i) \rightarrow A_\mu(\mathbf{r}_i) + \Delta_\mu/L_\mu$.

To study the behavior of the Ising-like domain walls we consider systems with sizes $L_x=L$, $L_y=L+1$, with L being

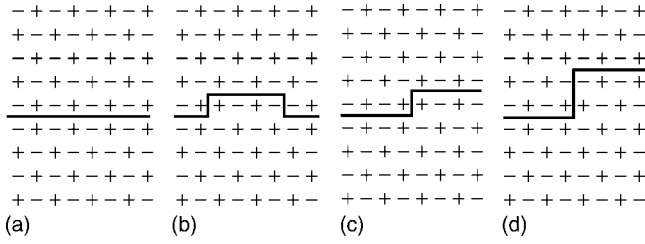


FIG. 1. Various configurations of the domain wall in a $L \times (L+1)$ system: (a) ground state, (b) finite width step of unit height (kink-antikink pair), (c) isolated kink of unit height, (d) isolated kink of height two. A (+) indicates the presence of a vortex in the XY model, or a charge $q_i=1/2$ in the dual Coulomb gas; a (-) indicates the absence of a vortex in the XY model, or a charge $q_i=-1/2$ in the dual CG. \hat{x} is the horizontal direction, and \hat{y} is the vertical direction.

even. The odd length L_y forces into the ground-state checkerboard pattern of vortices a single straight domain wall running the length of the system in the \hat{x} direction. This is illustrated in Fig. 1(a), where a (+) signifies a vortex in the phase angles $\theta(\mathbf{r}_i)$, and a (-) signifies the absence of a vortex.

Phase coherence in the FFX model is most conveniently studied by considering the dependence of the total free energy F on the total twist Δ_μ applied across the system [see Eq. (5)]. In a phase-coherent ordered state, we expect that $F(\Delta_\mu)$ varies with the twist Δ_μ ; in a phase-incoherent disordered state, we expect $F(\Delta_\mu)$ is independent of Δ_μ in the thermodynamic limit of $L \rightarrow \infty$. The dependence of the free energy on Δ_μ is readily obtained by using *fluctuating twist boundary conditions*,¹⁵ in which one treats the applied twist Δ_μ as a thermally fluctuating degree of freedom. If Z is the partition function for this ensemble, then the probability $P(\Delta_\mu)$ of finding a state with a particular twist Δ_μ is given by

$$P(\Delta_\mu) = \frac{e^{-F(\Delta_\mu)/T}}{Z}, \quad (6)$$

and so the free energy with respect to a reference twist $\Delta_{\mu 0}$ is

$$F(\Delta_\mu) - F(\Delta_{\mu 0}) = -T \ln [P(\Delta_\mu)/P(\Delta_{\mu 0})]. \quad (7)$$

The probability $P(\Delta_\mu)$ is directly measured within our fluctuating twist Monte Carlo simulation. We choose the reference twist $\Delta_{\mu 0}$ to be the value of the twist that minimizes the free energy $F(\Delta_\mu)$. For the gauge choice of Eq. (3), it is straightforward to see that the minimizing twist in the \hat{x} direction is at $\Delta_{x0}=0$. In our simulations we keep a fixed twist $\Delta_x=0$, and consider only the dependence of the free energy on the varying twist Δ_y , transverse to the Ising-like domain wall that is introduced in our $L \times (L+1)$ systems [see Fig. 1(a)]. In Fig. 2 we show sample results from our simulations for $F(\Delta_y) - F(0)$ vs Δ_y at two different values of $T < T_w$, for a system of size $L=128$. We see that $F(\Delta_y)$ has two equal minima at $\Delta_y=0$ and π (i.e., periodic and antiperiodic boundary conditions). One of these minima corresponds to states where the domain wall sits at even values of the height y , while the other corresponds to states where the domain wall sits at odd values of the height y . Below the kink-antikink unbinding transition T_w , the system is in a state of

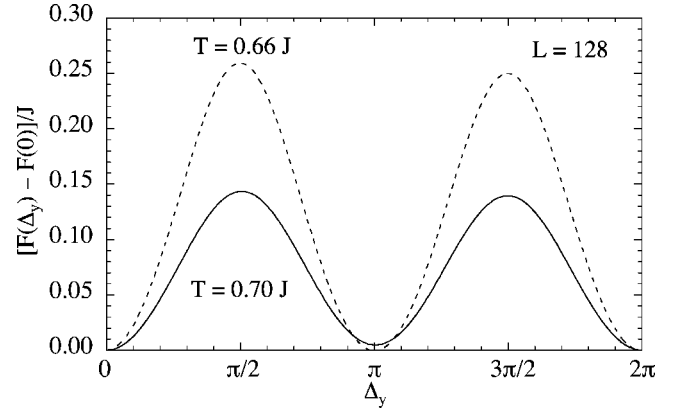


FIG. 2. Variation of total free energy F with total twist Δ_y applied transverse to the Ising-like domain wall, for two different temperatures in a system of size $L=128$.

broken translational symmetry; due to the free energy barrier between the two minima, states in which the domain wall is at an even height cannot be reached from states in which the domain wall is at an odd height. As noted by Korshunov,⁸ this broken symmetry is restored when phase coherence transverse to the wall is lost, i.e., when $F(\Delta_y)$ becomes independent of Δ_y , and so the free energy barrier between $\Delta_y=0$ and $\Delta_y=\pi$ vanishes. Alternatively viewed, when the domain wall changes its height by an odd number, the system acquires an average twist of π in the \hat{y} direction. Thus, restoring the symmetry of domain-wall translations leads to phase-angle fluctuations that destroy phase coherence transverse to the direction of the wall.

In our numerical work we will use two convenient measures of the variation of $F(\Delta_\mu)$ with Δ_μ . The first is the helicity modulus,^{2,14} Y_μ , which measures the curvature of $F(\Delta_\mu)$ at its minimum,

$$\begin{aligned} Y_\mu(L_x, L_y) &= \frac{L_\mu^2}{L_x L_y} \left. \frac{\partial^2 F}{\partial \Delta_\mu^2} \right|_{\Delta_\mu=0} \\ &= \frac{1}{L_x L_y} \left\{ \sum_i \langle V''(\phi_{i\mu}) \rangle_0 - \frac{1}{T} \left\langle \left[\sum_i V'(\phi_{i\mu}) \right]^2 \right\rangle_0 \right\}, \end{aligned} \quad (8)$$

where $\phi_{i\mu} \equiv \phi_\mu(\mathbf{r}_i) \equiv \theta(\mathbf{r}_i + \hat{\mu}) - \theta(\mathbf{r}_i) - A_\mu(\mathbf{r}_i)$, V' and V'' are the first and second derivatives of the Villain function of Eq. (4), and $\langle \dots \rangle_0$ indicates a thermodynamic average in the ensemble with fixed twist $\Delta_\mu=0$. A second measure is

$$\Delta F = F_{\max} - F_{\min} = F(\pi/2) - F(0), \quad (9)$$

where F_{\max} and F_{\min} are the maximum and minimum values of $F(\Delta_y)$, as Δ_y is varied at fixed $\Delta_x=0$. Since Y_μ is an intensive quantity, it should approach a value independent of system size as $L \rightarrow \infty$. The parameter ΔF scales as $Y(\Delta/L)^2 L^D$ in D dimensions, and so for $D=2$ it also becomes independent of system size as $L \rightarrow \infty$.

B. The Coulomb gas

Although our simulations are carried out in the XY variables $\theta(\mathbf{r}_i)$, it is helpful to consider the situation from the viewpoint of the dual CG model of logarithmically interacting half-integer charges.^{1,16} For the case of a fixed total twist Δ_μ , the XY Hamiltonian of Eq. (1) maps onto

$$\mathcal{H}_{CG} = \mathcal{H}_0 + \mathcal{H}_1. \quad (10)$$

\mathcal{H}_0 is the logarithmic interaction of the charges,

$$\mathcal{H}_0 = \frac{1}{2} (2\pi J) \sum_{i,j} q_i G(\mathbf{r}_i - \mathbf{r}_j) q_j, \quad (11)$$

where $q_i = \pm 1/2$ are the half-integer charges, neutrality is imposed, $\sum_i q_i = 0$, and $G(\mathbf{r})$ is the 2D periodic lattice Coulomb potential^{1,16} with $G(\mathbf{r}) \sim -\ln|\mathbf{r}|$ for large $1 \ll |\mathbf{r}| \ll L/2$. \mathcal{H}_1 arises from the fixed twist boundary condition and is given by^{17,18}

$$\mathcal{H}_1 = V_x \left(\Delta_x - A_x^0 + \frac{2\pi p_y}{L_y} \right) + V_y \left(\Delta_y - A_y^0 - \frac{2\pi p_x}{L_x} \right), \quad (12)$$

where V_x and V_y are Villain functions as in Eq. (4), but with couplings $J_x = J(L_y/L_x)$ and $J_y = J(L_x/L_y)$, respectively, and \mathbf{p} is the total dipole moment,

$$\mathbf{p} = \sum_i q_i \mathbf{r}_i, \quad (13)$$

and $A_x^0 = \sum_x A_x(x, y=0)$, $A_y^0 = \sum_y A_y(x=0, y)$. For the gauge choice of Eq. (3) we have

$$A_x^0 = 0, \quad A_y^0 = (L+1)\pi/2. \quad (14)$$

For the ground state as illustrated in Fig. 1(a), one has $p_y=0$, and so again it is easy to see from Eq. (12) that the total ground-state energy is minimized when $\Delta_x=0$. However, for this ground state one has $p_x=L/4$, hence the ground-state energy is minimized when $\Delta_y=(L+1)\pi/2 - \pi/2 = L\pi/2$. If the location of the domain wall were shifted by one unit in height, then the ground state would have $p_x=-L/4$, and the energy would be minimized when $\Delta_y=(L+1)\pi/2 + \pi/2 = L\pi/2 + \pi$. For L even, as we have required, these two values, modulus 2π , are just equal to 0 and π .

The helicity modulus Y_y/J maps^{3,14,15} onto the inverse dielectric function ϵ_x^{-1} of the CG. As noted by Korshunov,⁸ in order for the domain wall to move a unit lattice spacing in height, it must first form a unit step of finite width ℓ ; ℓ must be even to preserve charge neutrality [see Fig. 1(b)]. We denote the left-hand edge of the step as the *kink*, and the right-hand edge as the *antikink*. As the kink and antikink separate out to infinity, the domain wall moves one unit in height. As shown by Halsey,¹⁹ a corner in a domain wall carries with it a net charge of $\pm 1/4$. The kink, consisting of two successive corners with equal $+1/4$ charge, carries a net charge of $q_{\text{kink}} = +1/2$; the antikink carries a net charge of $q_{\text{antikink}} = -1/2$. At low temperatures, the logarithmic attraction between the kink and antikink charges keeps them bound with a largest separation $\ell_{\text{max}}(T)$. At higher temperatures,

entropy wins out over energy, and there is a kink-antikink unbinding transition at T_w , where $\ell_{\text{max}}(T_w) \rightarrow \infty$. Above T_w , the kink-antikink unbinding leads to diverging dipole fluctuations in the \hat{x} direction, driving ϵ_x^{-1} (and hence Y_y) to zero.

The problem of logarithmically interacting charges in one dimension (1D) has been treated by Bulgadaev.²⁰ Koshunov⁸ has applied these results to the unbinding transition of the kink-antikink pair along the one-dimensional Ising-like domain wall. To include the screening effect of charge excitations in the bulk of the system on either side of the Ising-like domain wall, we take as the coupling between kink-antikink pairs separated at a large distance to be the helicity modulus of the FFXY for an ordinary $L \times L$ system, $Y(L, L)$, in the limit of large enough L . Applying Bulgadaev's exact result for the unbinding transition temperature, we conclude

$$\frac{2\pi Y(L, L) q_{\text{kink}}^2}{T_w} = 2 \quad \text{or} \quad T_w = \frac{\pi}{4} Y(L, L). \quad (15)$$

One can reproduce this result using a Kosterlitz-Thouless-like argument³ as follows. In analogy with Lee *et al.*,¹¹ we consider the total free energy to have a single "free" (i.e., unbound) kink in the domain wall [see Fig. 1(c)]. Fixing the kink at a given position on the domain wall, its free energy (averaging over all other fluctuations) is that of an isolated $+1/2$ vortex in a medium with phase stiffness $Y(L, L)$; here we use Bulgadaev's result²⁰ that kink-antikink pairs in 1D do not lead to a renormalization of the kink-antikink interaction, and so any screening of their interaction is due to charge excitations in the bulk on either side of the domain wall, and so accounted for by the large L value of Y . As $L \rightarrow \infty$, the leading contribution to this energy is $E = \pi q_{\text{kink}}^2 Y \ln L$. The entropy of the kink is just that associated with its position along the domain wall, $S = -\ln L$. Combining gives $F_{\text{kink}} = E - TS = (\pi Y/4 - T) \ln L$, which as $L \rightarrow \infty$ gives the instability temperature for the formation of free kinks as $T_w = \pi Y/4$, in agreement with Eq. (15).

III. NUMERICAL RESULTS

A. Helicity modulus

We now present our numerical results. At each temperature, our simulations consist of typically $10^8 - 10^9$ ordinary MC passes through the entire lattice for the largest system sizes. In Figs. 3 and 4 we plot the helicity moduli Y_x and Y_y vs T , as computed by Eq. (8) in an ensemble with fixed twists $\Delta_x = \Delta_y = 0$. We show an "ordinary" case (no domain wall at $T=0$) of size 64×64 , which is large enough that any finite-size effects are negligible for the temperatures shown. In comparison, we also show several "anomalous" cases (percolating domain wall at $T=0$) of sizes $L \times (L+1)$. For the ordinary case, $Y_x = Y_y$, and the bulk transition (where the Y_μ jump discontinuously to zero in the thermodynamic limit) is⁶ at $T_{KT} \approx 0.81J$. In comparison, as L increases in the anomalous case, Y_x (parallel to the domain wall) in Fig. 3 approaches the value of the ordinary case, and so presumably vanishes at the same T_{KT} . However the curves of Y_y (trans-

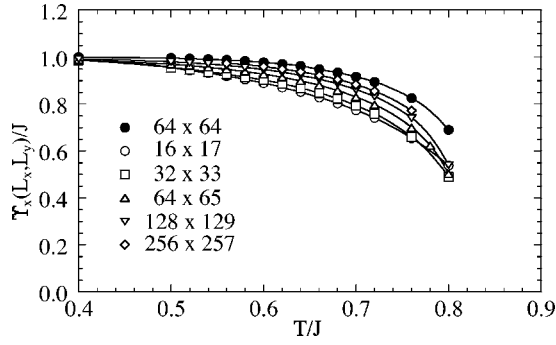


FIG. 3. Helicity modulus Y_x vs T for different system sizes $L_x \times L_y$. As $L \rightarrow \infty$, $Y_x(L, L+1)$ and $Y_x(L, L)$ approach the same curve.

verse to the domain wall) in Fig. 4 clearly decrease below that of the ordinary case and presumably vanish in the thermodynamic limit at a lower T_w .

The reduction seen in Y_y for the $L \times (L+1)$ systems, as compared to the $L \times L$ system, shown in Fig. 4, is due to the kinks at the Ising-like domain wall. To explicitly see this, we can consider the helicity modulus at the *finite wave vector*, $Y_y(k_x)$, defined as the response to a small sinusoidal perturbation in the vector potential $A_y(\mathbf{r}_i)$. If we take

$$A_y(\mathbf{r}_i) \rightarrow A_y(\mathbf{r}_i) + \sum_{k_x} \delta A_{k_x} e^{ik_x x_i} \quad (16)$$

then $Y_y(k_x)$ is defined by^{6,21}

$$Y_y(k_x) = \frac{1}{L_x L_y} \frac{\partial^2 F}{\partial \delta A_{k_x} \partial \delta A_{-k_x}} \Big|_{\delta A_{k_x}=0} \quad (17)$$

In view of the discussion following Eq. (5), equating the application of a uniform twist Δ_μ to the addition of a constant to the gauge field A_μ , the helicity modulus Y_y of Eq. (8) can also be viewed as the *zero wave vector* helicity $Y_y(k_x=0)$. In the CG representation, $Y_y(k_x)$ becomes the usual formula for the wave-vector-dependent inverse dielectric function,^{14,15}

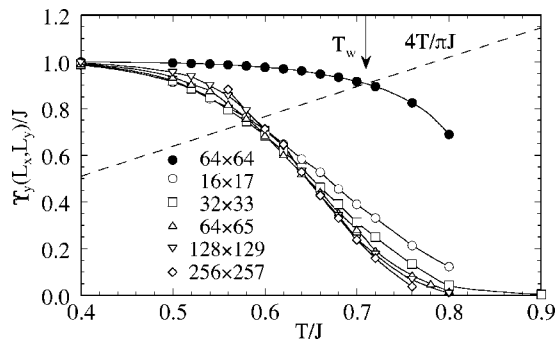


FIG. 4. Helicity modulus Y_y vs T for different system sizes $L_x \times L_y$. As $L \rightarrow \infty$, $Y_y(L, L+1)$ vanishes at a temperature lower than where $Y_y(L, L)$ vanishes. The intersection of the dashed line with $Y_y(L, L)$ indicates the kink-antikink unbinding temperature $T_w \approx 0.71J$ predicted by Eq. (15).

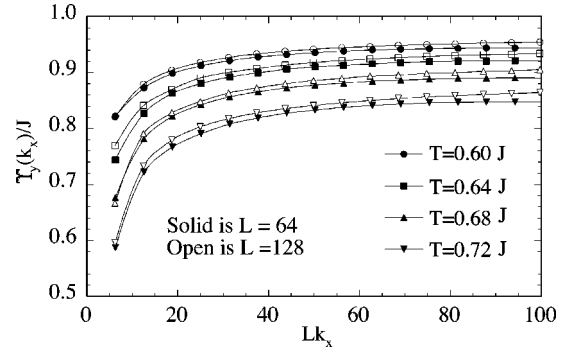


FIG. 5. Wave-vector-dependent helicity modulus $Y_y(k_x)$ vs Lk_x at several different temperatures T for system sizes $L \times (L+1)$, with $L=64$ (solid symbols) and $L=128$ (open symbols). The data for the different L collapse to a common curve at each T .

$$Y_y(k_x)/J = 1 - \frac{4\pi^2 J \langle q(k_x) q(-k_x) \rangle}{T L_x L_y k_x^2}, \quad (18)$$

where $q(\mathbf{k}) = \sum_i e^{i\mathbf{k} \cdot \mathbf{r}_i} q_i$ is the Fourier transform of the charge distribution.

Unlike Y_y of Eq. (8), which measures the response to a uniform twist applied at the boundaries, $Y_y(k_x)$ measures the response to a spatially varying twist applied throughout the bulk of the system. For a homogeneous system with *periodic boundary conditions*, one in general expects $Y_y = \lim_{k_x \rightarrow 0} Y_y(k_x)$, since the spatially varying twist becomes uniform as $k_x \rightarrow 0$, and $\delta A_{k_x} \rightarrow \Delta_y/L_y$. For *free boundary conditions*, however, where the phase angle $\theta(x, L_y)$ is not coupled to the phase angle $\theta(x, 0)$, this equality does not hold. For free boundary conditions, the absence of any constraint [such as in Eq. (5)] relating $\theta(x, L_y)$ to $\theta(x, 0)$ means that the phase angles are free to untwist any additive constant to the gauge field, $A_y(\mathbf{r}_i) \rightarrow A_y(\mathbf{r}_i) + \Delta_y/L_y$, by choosing $\theta(x, y+1) - \theta(x, y) = \Delta_y/L_y$; hence, if one computes Y_y by Eq. (8) in a free boundary ensemble, one necessarily has $Y_y = 0$ at any temperature. For the spatially varying twist of Eq. (16), however, no such transformation is possible since the perturbing twist is a strictly transverse vector function, while the phase angle differences give a strictly longitudinal vector function. In this case one finds that $\lim_{k_x \rightarrow 0} Y_y(k_x)$ has the same value, as $L \rightarrow \infty$, that one has for the system with periodic boundary conditions.

We expect a similar effect to be true in our present case. The kink-antikink pairs confined to the one-dimensional Ising-like domain wall can be viewed as a relaxation of the boundary condition. They can unwind, or soften, the energy of a uniform twist Δ_y applied at the boundary, but cannot unwind a spatially varying twist δA_{k_x} applied throughout the bulk of the system. We therefore expect that, as $L \rightarrow \infty$, $\lim_{k_x \rightarrow 0} Y_y(k_x)$ will equal the value of Y_y obtained for an ordinary $L \times L$ system, representing the stiffness of the bulk of the system on either side of the domain wall; Y_y , however, will be a lower value including effects due to the polarization of the kink-antikink pairs localized to the domain wall.

In Fig. 5 we plot, at several different temperatures around T_w , $Y_y(k_x)$ for finite k_x for $L \times (L+1)$ systems with sizes

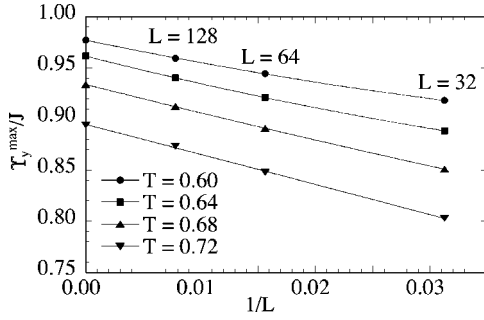


FIG. 6. $Y_y^{\max} \equiv \max_{k_x} [Y_y(k_x)]$ vs $1/L$ at several different temperatures T . The values at $1/L=0$ correspond to Y_y for an ordinary 64×64 system. Solid lines are fits to a quadratic polynomial.

$L=64$ and 128 . When we plot the results versus the scaled axis of Lk_x , we see that the data for the two different system sizes collapse to essentially a common curve, $u(Lk_x)$, at each temperature. As $L \rightarrow \infty$, such scaling implies that $\lim_{k_x \rightarrow 0} [\lim_{L \rightarrow \infty} Y_y(k_x)] = \lim_{\kappa \rightarrow \infty} u(\kappa)$ is different from Y_y , just as we have argued. We may estimate $\lim_{\kappa \rightarrow \infty} u(\kappa)$ by taking the maximum value of $Y_y(k_x)$ for each system size L . In Fig. 6 we plot $Y_y^{\max} \equiv \max_{k_x} [Y_y(k_x)]$ versus $1/L$ for the same temperatures as shown in Fig. 5. We give results for $L=32, 64$, and 128 . At $1/L=0$ we plot the value of $Y_y(L, L)$ for $L=64$, representing the large L limit for the helicity modulus of the ordinary system without the Ising domain wall. We see that the values of Y_y^{\max} extrapolate perfectly to $Y_y(L, L)$ as $1/L \rightarrow 0$. This confirms the following conclusion. As $L \rightarrow \infty$ in an $L \times (L+1)$ system, the finite wave-vector helicity $Y_y(k_x)$ is equal to the corresponding helicity modulus of an ordinary $L \times L$ system for *all* finite values of k_x ; this measures the stiffness of the bulk of the system on either side of the Ising domain wall, and it is unaffected by the kinks on the wall. However the zero wave-vector response Y_y to a uniform twist Δ_y , shown in Fig. 4, is softened and above T_w reduced to zero—by the polarization of the kinks on the domain wall.

B. Finite-size dependence

Returning to Fig. 4, we have indicated the kink-antikink unbinding transition temperature T_w , as predicted in Eq. (15), by the intersection of the line $4T/\pi J$ with the helicity modulus of the ordinary $L \times L$ system. This gives an estimate of $T_w \approx 0.71J$. This value occurs noticeably above the point where many of the curves $Y_y(L, L+1)$ appear to cross. Such a crossing point, if remaining constant as L increases, is generally taken as an estimate for the phase transition in a 2D XY system. To explain the difference between this crossing point at $\sim 0.60J$ and the above estimate $T_w \approx 0.71J$, we need to examine the finite-size dependence of $Y_y(L, L+1)$ more carefully.

To get the most accurate results, we have found it better to work in the fluctuating twist ensemble and compute the phase-coherence parameter ΔF of Eq. (9), rather than work with periodic boundary conditions and measure Y_y . In Fig. 7 we plot our results for ΔF versus system size $1/L$ for various temperatures T above and below T_w . We use $L \times (L+1)$ sys-

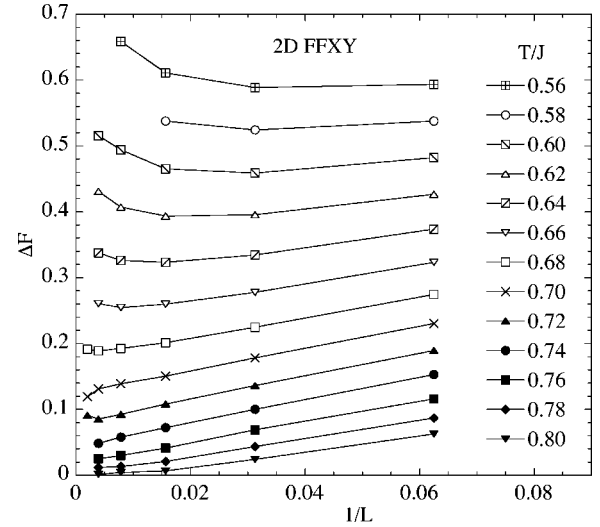


FIG. 7. ΔF of Eq. (9) vs $1/L$ at various temperatures for the 2D FFXY model of size $L \times (L+1)$.

tems with L ranging from 32 up to 512. We note that at low T , the behavior of ΔF is *nonmonotonic*; as L increases, the system first softens with a decreasing ΔF , but then stiffens again as ΔF reaches a minimum and then increases. We denote the system size at this minimum by ξ_k . Since the system becomes stiffer on length scales $L > \xi_k$, we assume that ξ_k determines the size of the largest kink-antikink pairs on the domain wall. At higher T , the minimum in ΔF disappears, and ΔF continues to decrease as L increases. The temperature that separates the two behaviors is somewhere between $0.68J$ and $0.74J$, in good agreement with the result $T_w \approx 0.71J$ from Fig. 4, based on the theoretical prediction of Eq. (15).

As a further check on our results, we have also directly simulated a one-dimension (1D) neutral system of logarithmically interacting charges $q_{\text{kink}} = \pm 1/2$. The 1D interaction potential is taken as the 2D $L \times L$ lattice Coulomb potential, as in Eq. (11), but with the height separation fixed at $y=0$. We use an interaction coupling constant of $2\pi Y_y(L, L)$, with $Y_y(L, L)$ obtained from our simulations of the ordinary $L \times L$ 2D FFXY model for $L=64$, in order to model as closely as possible the interaction between kinks on the domain wall in the true $L \times (L+1)$ FFXY model system. Within this 1D simulation we measure the normalized histogram of the total dipole moment, $P(p_x)$, and use it to construct²² what would be the free energy $F(\Delta_y)$ of the corresponding $L \times (L+1)$ 2D FFXY system,

$$F(\Delta_y) = -T \ln \left[\sum_{p_x} P(p_x) e^{-V_y[\Delta_y - A_y^0 - (2\pi p_x/L)]/T} \right] + \text{const}, \quad (19)$$

where V_y is the Villain function as in Eq. (12), and “const” is a constant term independent of Δ_y .

In Fig. 8 we plot the resulting $\Delta F = F(\pi/2) - F(0)$ versus $1/L$ for the same temperatures and sizes L as in Fig. 7. The agreement between Figs. 7 and 8 is not exact, since the coupling between kinks is only equal to $2\pi Y_y(L, L)$

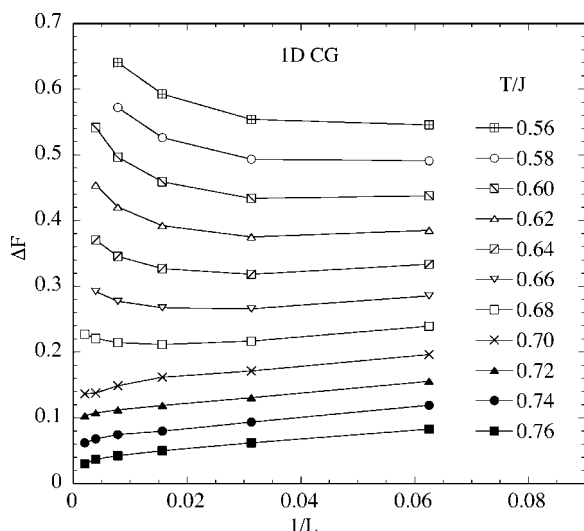


FIG. 8. ΔF of Eq. (9) vs $1/L$ at various temperatures as estimated from the dipole histogram of a 1D interacting kink model (see text).

on large length scales; the true screening of the kink interaction due to charge excitations in the bulk on either side of the domain wall is length scale dependent. Moreover, the domain wall in the 2D FFX model is not a strictly straight one-dimensional line; the roughness of the domain wall (see the following section) means that height fluctuations can add to the distance of separation between kinks. Nevertheless, the agreement is qualitatively very good, indicating again that it is the polarization of kink-antikink pairs along the Ising domain wall that is responsible for the decrease in the phase stiffness transverse to the domain wall.

One evident feature of both Figs. 7 and 8 is the very large finite-size effect. The asymptotic behavior of ΔF only sets in at quite large length scales. Equivalently, the correlation length of the kink-antikink pairs, ξ_k , grows large well below $T_w \approx 0.71J$. Fitting the data of Fig. 7 to a quadratic in $\ln L$, and determining ξ_k from the minima of these fitted curves, we plot the resulting ξ_k versus T in Fig. 9. The rapidly growing ξ_k means that it is difficult to get a very precise estimate of T_w directly from the data of Fig. 7, without going to prohibitively large system sizes $L \gg 512$. We believe that this is also the reason that Lee *et al.*¹¹ report a lower value²³ of $T_w/J = 2\pi(0.09 \pm 0.01) = 0.57 \pm 0.06$ for the “roughening transition” temperature in their dual 2D Coulomb gas. The simu-

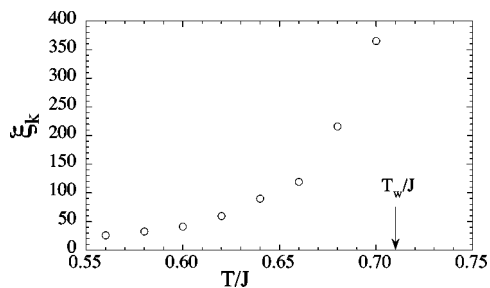


FIG. 9. Kink-antikink correlation length ξ_k vs T , obtained from the data of Fig. 7.

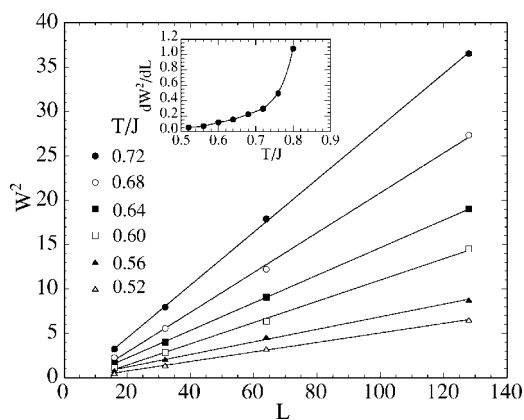


FIG. 10. Domain-wall width squared, W^2 , vs L for several different T . Straight lines are linear fits, showing rough domain walls at all T , even below $T_w \approx 0.71J$. The inset shows the slopes of the curves, dW^2/dL , vs T .

lations of Lee *et al.* are on a lattice of size $L=64$. From Fig. 9 we see that $\xi_k \sim 32$ at $T/J \sim 0.58$, hence kinks already look unbound above this temperature for such a small system size. The large values of ξ_k can also be compared to other length scales in the system. The correlation length of the Ising-like order parameter, ξ_l , gives the typical size of an Ising-like domain excitation in an ordinary $L \times L$ FFX model. From Ref. 6 (see Fig. 15) we find that ξ_l is quite small below $T_w \approx 0.71J$, in particular $\xi_l < 2.5$ for $T < 0.77J$. Thus we expect that kink-antikink pairs on the domain wall enclosing a typical thermally excited Ising-like domain are always effectively unbound. The energetics of kink-antikink unbinding will only effect the morphology of domains that are much larger than those due to typical thermal excitations.

C. Roughening

Finally, we consider the roughness of the domain wall. As noted by Koshunov,⁸ an isolated step on a domain wall of height 2 [see Fig. 1(d)] carries no net charge, each corner giving opposite $1/4$ charges that therefore cancel. Such isolated height of 2 steps therefore cost finite energy, and should roughen the domain wall at any finite temperature. To verify this we have explicitly measured the domain-wall width squared,

$$W^2 = \frac{1}{N_s} \sum_s \langle (y(s) - \bar{y})^2 \rangle, \quad (20)$$

where s is an index that counts horizontal length traveled along the domain wall ($s=x$ if there are no overhangs), $y(s)$ is the height of the domain wall at index s , \bar{y} is the average height of the domain wall in the particular configuration, and N_s is the number of horizontal links in the domain wall ($N_s=L$ if there are no overhangs). To avoid problems with periodic boundary conditions, we always measure the domain wall height as relative to some initial starting position. In Fig. 10 we plot W^2 vs L for various temperatures. The linear growth in W^2 as L increases indicates that the domain wall is rough for all temperatures shown, including $T < T_w$.

The domain-wall diffusion constant, dW^2/dL , shows no observable singularity at $T_w \approx 0.71J$ (see the inset to Fig. 10).

IV. DISCUSSION

Our numerical results demonstrate the existence of the unbinding transition for kink-antikink pairs along the domain wall of Ising-like excitations in the 2D FFX model and that the behavior of this transition is in good agreement with the theoretical predictions of Korshunov.⁸ We show that domain walls are rough at all temperatures, and therefore argue that the “roughening transition” claimed by Lee and co-workers^{10,11} is really the kink-antikink unbinding transition. We show that the effects of kink-antikink pairs are not readily apparent for Ising-like domains, such as are typically present due to thermal excitation; because of the large length ξ_k , such effects are important only for much larger domains.

One of Korshunov’s main motivations for investigating the kink-antikink unbinding transition was to argue that such a transition necessarily implies the existence of two separate bulk transitions, $T_{KT} < T_I$. We now present our own thoughts on this issue. In the original paper by Teitel and Jayaprakash,² two possibilities were considered, $T_{KT} < T_I$ and $T_{KT} = T_I$. In discussing the first case, Teitel and Jayaprakash presented the following scenario. In terms of the dual CG model, the helicity modulus Y gets reduced from its $T=0$ value by fluctuations that produce dipole moments. If Ising domains of typical size ξ_l carried a total dipole moment proportional to their size, they would drive $Y \rightarrow 0$ continuously, due to the diverging ξ_l as $T \rightarrow T_I$ from below. However, in addition to these domain excitations, there are also pair excitations. The original Kosterlitz-Thouless instability criteria would imply that pairs unbind once Y falls below the critical value $Y(T) = 2T/\pi$, which must happen at some T_{KT} below T_I . However, if one computes domain energies at $T=0$ (and presumably the same holds for domain free energies at low T), one finds that it is only the domains with *vanishing* total dipole moment that have energies which scale with the perimeter; i.e., the only domains which are “Ising-like” are

those which carry no dipole moment and so cannot give any reduction in Y . Fortunately, once T increases above T_w , kink-antikink pairs on the boundary of the domain are free to unbind, and the Ising domains can now acquire large dipole moments at no cost in free energy. The scenario of Teitel and Jayaprakash is now restored. This conclusion is in complete agreement with the numerical work of Olsson,^{5,6} who finds two distinct transitions at $T_{KT} < T_I$, and argues that the non-Ising-like critical behavior claimed by some⁷ at T_I is in fact an artifact of finite size effects.

The kink-antikink unbinding transition may also have implications for the nonequilibrium steady state behavior of the system when the vortices are driven by a uniform force, such as is the case for a fully frustrated Josephson junction array in an applied uniform dc current I . Since I couples linearly to the total dipole moment of a domain p , the force can lead to an instability²⁴ in domain growth, provided the free energy of exciting the domain scales less than linearly with p . For $T < T_w$, the binding of kinks to antikinks prevents large dipole moments from building up on domains. The Ising-like domains, whose free energy scales like the domain length ℓ , are only those domains whose total dipole moment vanishes, and, hence, these domains remain stable, and the Ising-like order should persist at small drives. For $T > T_w$, kink-antikink pairs can unbind, resulting in domains whose dipole moment may scale at least proportional to their length ℓ . In this case, when the current exceeds an amount proportional to the Ising domain surface tension, domains will become unstable to growth and the Ising-like order will be destroyed.

ACKNOWLEDGMENTS

We wish to thank S. E. Korshunov for his very helpful correspondence and comments on an earlier version of this manuscript. This work was supported by the Engineering Research Program of the Office of Basic Energy Sciences at the Department of Energy Grant No. DE-FG02-89ER14017 and the Swedish Research Council Contract No. 2002-3975. Travel between Rochester and Umeå was supported by Grants Nos. NSF INT-9901379 and STINT 99/976(00).

¹J. Villain, J. Phys. C **10**, 1717 (1977); **10**, 1793 (1977).

²S. Teitel and C. Jayaprakash, Phys. Rev. B **27**, 598 (1983).

³J. M. Kosterlitz and D. J. Thouless, J. Phys. C **5**, L124 (1972); **6**, 1181 (1973).

⁴S. Lee and K.-C. Lee, Phys. Rev. B **49**, 15184 (1994); V. Cataudella and M. Nicodemi, Physica A **233**, 293 (1996); Y. Ozeki and N. Ito, Phys. Rev. B **68**, 054414 (2003).

⁵P. Olsson, Phys. Rev. Lett. **75**, 2758 (1995); **77**, 4850 (1996).

⁶P. Olsson, Phys. Rev. B **55**, 3585 (1997).

⁷M. Yosefin and E. Domany, Phys. Rev. B **32**, 1778 (1985); B. Berge, H. T. Diep, A. Ghazali, and P. Lallemand, *ibid.* **34**, 3177 (1986); J. Lee, J. M. Kosterlitz, and E. Granato, *ibid.* **43**, R11531 (1991); E. Granato and M. P. Nightingale, *ibid.* **48**, 7438 (1993); G. Ramirez-Santiago and J. V. José, *ibid.* **49**, 9567 (1994); E. H. Boubcheur and H. T. Diep, *ibid.* **58**, 5163 (1998).

⁸S. E. Korshunov, Phys. Rev. Lett. **88**, 167007 (2002).

⁹M. Y. Choi and S. Doniach, Phys. Rev. B **31**, 4516 (1985); E. Granato, J. M. Kosterlitz, J. Lee, and M. P. Nightingale, Phys. Rev. Lett. **66**, 1090 (1991); J. Lee, E. Granato, and J. M. Kosterlitz, Phys. Rev. B **44**, 4819 (1991); M. P. Nightingale, E. Granato and J. M. Kosterlitz, *ibid.* **52**, 7402 (1995).

¹⁰S. J. Lee, J.-R. Lee, and B. Kim, Phys. Rev. E **51**, R4 (1995).

¹¹J.-R. Lee, S. J. Lee, B. Kim, and I. Chang, Phys. Rev. Lett. **79**, 2172 (1997).

¹²G. S. Jeon, S. J. Lee, and M. Y. Choi, Phys. Rev. B **67**, 014501 (2003).

¹³J. Villain, J. Phys. (Paris) **36**, 581 (1975).

¹⁴T. Ohta and D. Jasnow, Phys. Rev. B **20**, 139 (1979).

¹⁵P. Olsson, Phys. Rev. B **52**, 4511 (1995).

¹⁶J. V. José, L. P. Kadanoff, S. Kirkpatrick, and D. R. Nelson, Phys.

- Rev. B **16**, 1217 (1977).
- ¹⁷A. Vallat and H. Beck, Phys. Rev. B **50**, 4015 (1994).
- ¹⁸H. S. Bokil and A. P. Young, Phys. Rev. Lett. **74**, 3021 (1995).
- ¹⁹T. C. Halsey, J. Phys. C **18**, 2437 (1985).
- ²⁰S. A. Bulgadaev, Phys. Lett. **86A**, 213 (1981); Teor. Mat. Fiz. **51**, 424 (1982) [Theor. Math. Phys. **51**, 593 (1982)].
- ²¹P. Minnhagen, Rev. Mod. Phys. **59**, 1001 (1987).
- ²²P. Gupta, S. Teitel, and M. J. P. Gingras, Phys. Rev. Lett. **80**, 105 (1998).
- ²³We have converted temperature scales between the CG model of Ref. 11 and our FFXY model, $T_{XY}=2\pi T_{CG}$.
- ²⁴K. K. Mon and S. Teitel, Phys. Rev. Lett. **62**, 673 (1989).